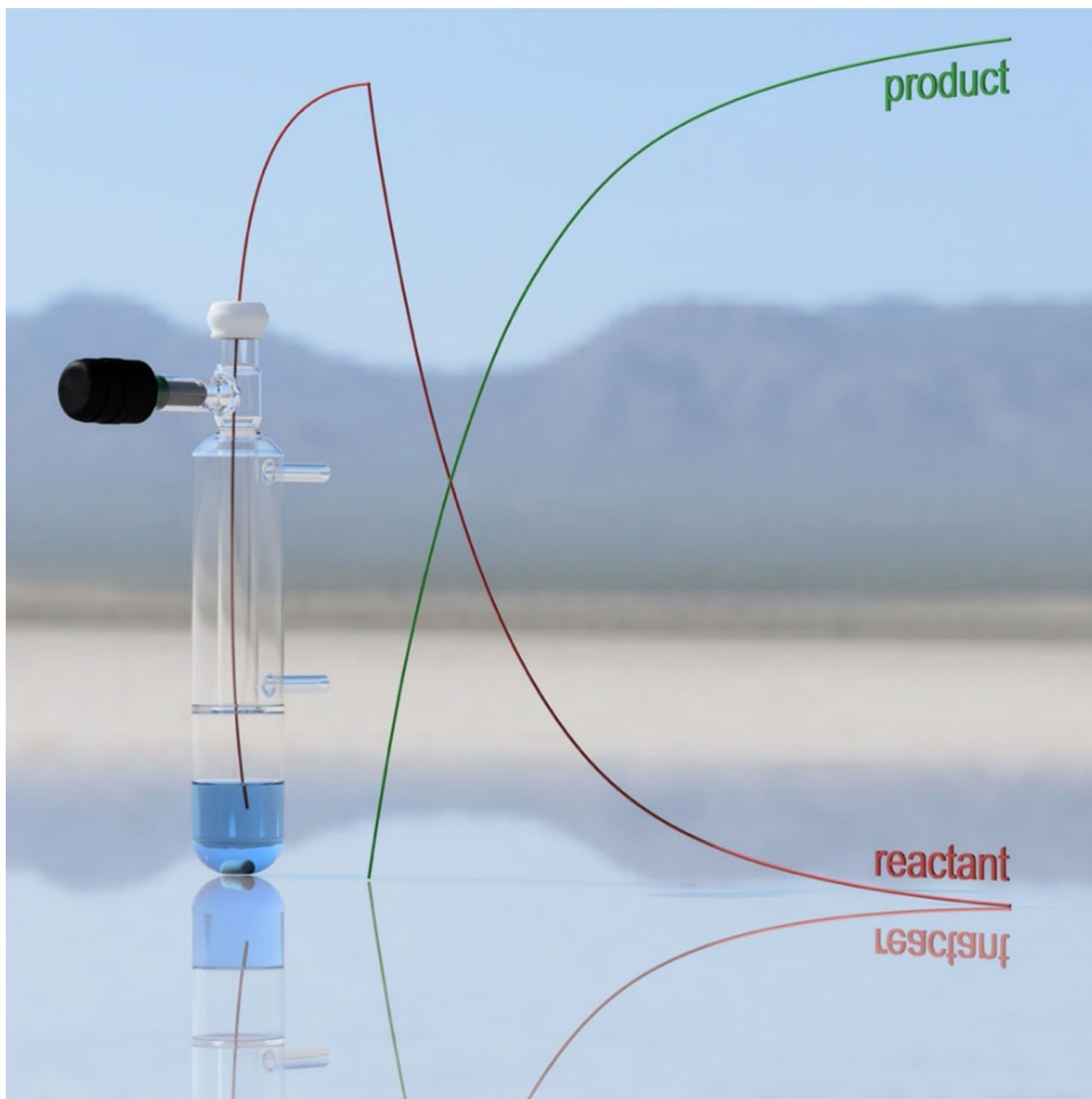




# Pressurized Sample Infusion

Gilian T. Thomas, Sofia Donnecke, Ian C. Chagunda, and J. Scott McIndoe\*<sup>[a]</sup>



Pressurized sample infusion (PSI) is a simple and effective means of continuously introducing a solution to an electrospray ionization mass spectrometry (ESI-MS) source. It allows for acquisition of real-time data in an air- and moisture-free environment and requires minimal additional infrastructure. It is applicable for use for any reaction in which one or more

components are detectable by ESI-MS and for which time-course information is desired over a time scale of seconds to minutes. The strengths and weaknesses of the method are critically examined, and technique tips and tricks are provided to enable maximal effectiveness when employing this approach to continuous monitoring of complex reaction mixtures.

## 1. Introduction

Real-time reaction monitoring does not necessarily mean rapid or in situ analysis, though it can involve both; it simply means a type of analysis that allows the experimenter to probe the reaction as it is happening and make decisions about how to proceed, for example, when to add the next reagent, when to increase the temperature, when to add more catalyst, or when to stop the reaction as it comes to completion. An off-line technique can be used in a real-time sense if the reaction is sufficiently slow; however, most of the examples in this review will focus on techniques that provide results to the chemist monitoring the reaction on a time frame of seconds and minutes.

High Performance Liquid Chromatography (HPLC) is a common method of reaction monitoring as it provides data density as well as deconvolution of reaction components. Additionally, it is compatible with several detection methods such as UV-Vis spectroscopy, fluorimetry, and evaporative light scattering.<sup>[1]</sup> This method of reaction monitoring, however, is considered off-line as aliquots must be withdrawn from the reaction solution at specified time intervals and subsequently injected into the HPLC. On-line dilution of process level concentrations has been achieved by Hein and coworkers such that the aliquot is withdrawn from the reaction vessel and diluted in-line prior to injection on to the HPLC column.<sup>[2]</sup> HPLC has also been adapted to accommodate air-sensitive reaction monitoring through the use of a glovebox.<sup>[3]</sup>

Nuclear Magnetic Resonance (NMR) spectroscopy offers real-time data acquisition when equipped with a flow system<sup>[4,5]</sup> or a stopped-flow system.<sup>[6–8]</sup> This allows for reaction intermediates to be observed, provided they are not short-lived and produced in high enough concentrations. Physical factors, such as consistent mixing and flow rates of these systems, are the key to maintaining quality data. In most cases, a protic solvent will be used rather than a deuterated solvent to ensure the reaction conditions are as realistic as possible; however, this can

lead to data convolution if the instrument is not equipped to handle protic solvents.<sup>[9]</sup>

Mass Spectrometry (MS) offers a complementary data set to NMR spectroscopy as it provides data on charged intermediates that may be short-lived and/or generated at low concentrations. Additionally, MS is capable of detecting radical intermediates and paramagnetic metal complexes, an area where NMR spectroscopy has weaknesses.<sup>[10–12]</sup>


HPLC is one of the most common ways of introducing samples into the mass spectrometer as it separates analytes by flowing through a column and allows for small volume injections.<sup>[13]</sup> Syringe pumps may also be used as they are compatible with a multitude of solvents and facilitate sample introduction at a set flow rate (typically lower than HPLC flow rates); however, in terms of reaction monitoring, temperature and solution mixing are relatively uncontrollable.<sup>[14]</sup> Mass spectrometers may be connected to a microreactor; however, each data point is collected in a separate experiment, and to accommodate higher reaction times, longer tubing is used.<sup>[15,16]</sup> A pressurized sample injection bomb apparatus capable of cleanup has been described with pneumatic control.<sup>[17]</sup> Flow injection systems have also been developed to facilitate sample delivery on a  $\text{nL min}^{-1}$  and  $\mu\text{L min}^{-1}$  scale enabling injection of up to 1200 samples per day without carryover.<sup>[18]</sup>


In terms of air- and moisture-free sample introduction, some techniques have been described whereby a nitrogenous atmosphere is either attached to the MS source, such as a glove bag<sup>[19,20]</sup> and a small glove chamber.<sup>[21]</sup> On a larger scale, a glovebox can be modified to accommodate a feedthrough port for tubing going directly into the MS source.<sup>[22,23]</sup> The need for a simple, cheap, robust method of air- and moisture-free sample introduction was obvious, hence the development of Pressurized Sample Infusion (PSI).<sup>[24]</sup>

## 2. Description of the Method

First reported in 2010, Pressurized Sample Infusion (PSI) is a sample introduction method providing on-line reaction monitoring of reaction solutions.<sup>[24]</sup> It is essentially a positive pressure cannula transfer<sup>[25]</sup> of a reacting solution directly into an electrospray ionization mass spectrometer (ESI-MS). It does not require mechanical pumping, and infuses a raw reaction mixture without further treatment. ESI-MS is a technique limited to the analysis of species that carry a charge or are readily able to acquire one (e.g., a molecule with a basic site that can associate with a proton or an alkali metal ion) since it is capable of detecting only ions pre-formed in solution. It is also best suited to species present at very low concentration. With those

[a] Dr. G. T. Thomas, S. Donnecke, I. C. Chagunda, Prof. Dr. J. S. McIndoe  
Department of Chemistry, University of Victoria  
PO Box 1700 STN CSC  
Victoria, BC V8W 2Y2 (Canada)  
E-mail: mcindoe@uvic.ca

 Supporting information for this article is available on the WWW under <https://doi.org/10.1002/cmtd.202100068>

 © 2021 The Authors. Published by Wiley-VCH GmbH. This is an open access article under the terms of the Creative Commons Attribution Non-Commercial NoDerivs License, which permits use and distribution in any medium, provided the original work is properly cited, the use is non-commercial and no modifications or adaptations are made.

two principal restrictions in mind, ESI-MS is especially well suited to systems involving charged catalysts.<sup>[26]</sup> When a charged catalyst is not an option, charged-tags are often used to apply a charge to a species of interest, with the reactivity of these charged-tags observed using PSI-ESI-MS.<sup>[27–29]</sup>

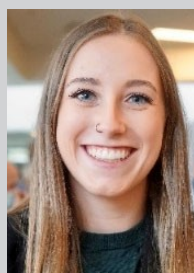
In terms of concentration limitations, the level of response yielded by ESI-MS is dictated by the nature of the analyte under study. For anything that carries a permanent charge, concentrations should be kept to low millimolar and below. If that species is also lipophilic and rigid (i.e., highly surface-active and hence prone to be disproportionately found on the surface of the sprayed droplets and overrepresented in the mass spectrum),<sup>[30]</sup> that concentration should be micromolar or lower. Species that are not charged can generally be run at higher concentrations, but such species exhibit variability not just in surface activity but also in extent of ionization.<sup>[31–40]</sup> Bases can be readily protonated and acids deprotonated, giving good response factors, but neutral molecules lacking any such sites will generally be invisible to ESI-MS. The addition of a tee piece connector can also be added to dilute the concentration of solution injected;<sup>[41,42]</sup> however, this may not represent reaction pathways present at industrial level concentrations. At higher concentration levels, flow/stopped-flow NMR spectroscopy may be a more suitable technique.

ESI-MS solvents need to be reasonably polar in order to enable the electrochemistry that creates the excess charge for the ESI process.<sup>[43]</sup> Non-polar solvents are widely known as incompatible with ESI-MS due to their low conductivity; however, addition of a lipophilic ionic liquid (a supporting electrolyte) can overcome this problem.<sup>[43]</sup> Aspects to take into consideration if using an ionic liquid to facilitate ESI performance: (1) it must be unreactive towards any of the reaction components, and (2) it should not overlap with any signals of interest.

The PSI approach works at temperatures up to the boiling point of the solvent. Temperatures higher than the boiling point will overpressurize the flask. PSI can operate at lower temperatures than ambient; however, unless insulated tubing is used, the utility of this is limited by the fact that the tubing and ESI source will be at room and elevated temperature, respectively, and so the reaction will be briefly exposed to these raised temperatures. As such, temperatures below 0 °C are not recommended unless the reaction of interest is relatively slow.

PSI is conducted at slightly above ambient pressure, by 2–5 psi (0.14–0.34 bar). More highly pressurized systems are not recommended without use of a pressure vessel with the appropriate safety features (and a narrower diameter tubing to decrease the flow rate to something compatible with ESI-MS). Regulated tanks of N<sub>2</sub> or Ar are commonly used to deliver the positive pressure to the flask, though other options are available. Using a balloon filled with gas, samples can be prepared on a Schlenk line and then safely transferred to the mass spectrometer for sample introduction.<sup>[44]</sup> This method also introduces more versatility to the PSI technique as any gas can be used to fill the balloon. A single balloon supplies about 1 psi; double-walled balloons can provide increased pressure if required. In reactions where volatile side products are formed, the pressure generated is insignificant relative to pressure changes effected by increasing the temperature due to the small scale of the reaction. Flow rate into the mass spectrometer is primarily important in extreme cases; for example, low flow rates can cause sputtering and erratic flow, and high flow rates can lead to flooding of the source.

PSI-ESI-MS is most useful for providing temporal intensity profiles for every charged component of the reaction.<sup>[45]</sup> These profiles correspond to reactant, product, pre-catalyst, catalyst and reaction impurities, intermediates, decomposition products, and resting states (Figure 1). Based on the behaviour of analytes



Gilian Thomas recently defended her Ph.D. dissertation at the University of Victoria. She received her M.Sc. in analytical chemistry at Carleton University before joining the McIndoe group. Her Ph.D. research has focused on reaction monitoring using mass spectrometry, and her post-doctoral research will be focused in the area of process chemistry.



Sofia Donnecke is currently in the fourth year of her PhD program at the University of Victoria. She completed her undergraduate degree at Harvard University in 2018 in chemistry with a minor in Earth and Planetary Science. Her current research focuses on understanding organometallic reaction pathways using computational methods as well as ESI-MS.



Ian Chagunda is a 2nd year Ph.D. student at the University of Victoria in the McIndoe lab. His research is focused on mechanistic investigations of palladium catalyst activation and carbon-carbon bond formation reactions using pressurized sample infusion electrospray ionization mass spectrometry (PSI ESI-MS). He is a B.Sc. graduate of Simon Fraser University, working as an NSERC undergraduate researcher under the supervision of Dr. Charles Walsby on the synthesis of bimetallic ruthenium and platinum complexes as targets for enhanced anti-cancer activity.



Scott McIndoe was educated in New Zealand at the University of Waikato and was a postdoctoral research fellow and college lecturer at the University of Cambridge (UK) before moving to his current position at the University of Victoria (Canada) in 2003. His research team investigate challenging inorganic and organometallic catalytic systems using characterization tools and methodologies of their own devising, and mass spectrometry plays a central role in their studies.

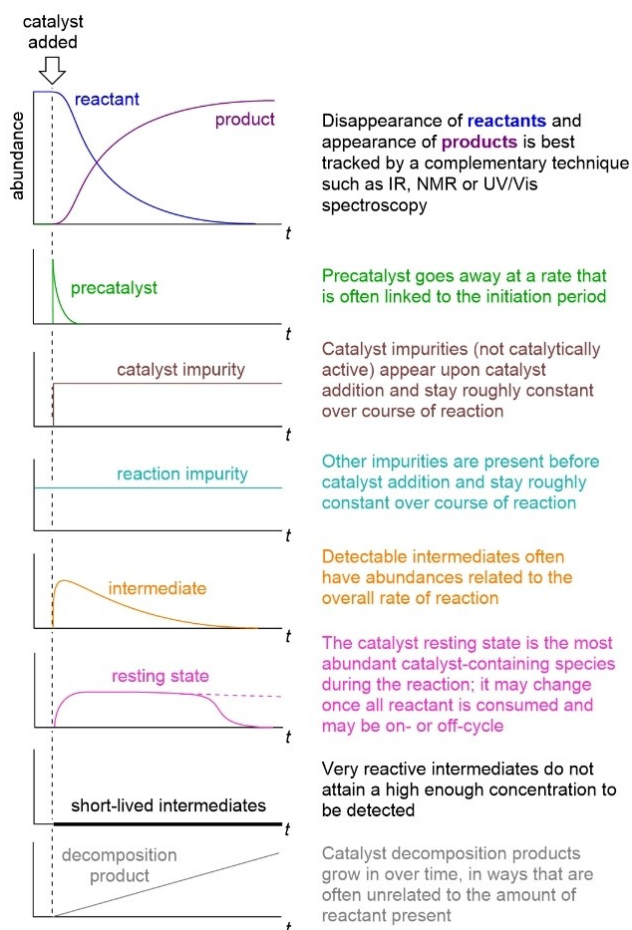


**Figure 1.** Idealized temporal profiles for different reaction components over the course of a reaction. These dynamics provide important clues as to which reaction role a given species is most likely playing. Adapted with permission from Ref. [45]. Copyright 2016, American Chemical Society.

over time, their role in the reaction can be defined. This sample introduction method becomes even more powerful when combined with computation, which can provide further structural information and bond dissociation energies.<sup>[46,47]</sup>

The ability to acquire data on catalyst resting state and overall reaction progress simultaneously is a significant advantage of the technique and can be improved further through combination with orthogonal methods. Because MS is so sensitive, it is generally best suited to analyze reaction components at low concentration (e.g., species related to the catalyst) while the orthogonal method takes care of overall reaction progress by tracking the disappearance of reactant(s) and/or appearance of product(s). Flow Infrared Spectroscopy (IR) is an ideal candidate for this type of analysis (Figure 2).<sup>[45]</sup>

There is some dead time between the solution leaving the flask and arriving in the mass spectrometer, in the order of 5–20 s. Variables here include the viscosity of the solvent, the inner diameter of the tubing, the length of the tubing and the applied pressure. An estimate of flow rate can be established using the Hagen-Poiseuille equation.<sup>[48,49]</sup> This dead time sets a lower bound for establishing reaction rates to a  $t_{1/2}$  of 20 s or

more. The upper bound is set only by practical limitations such as the volume of solvent available (solvent is consumed at typical rates of 5–20  $\mu\text{L min}^{-1}$ ), the booking of instrument time, and the increased likelihood of clogging and instrumental contamination from an extended analytical run. In practice, optimal results are obtained by running experiments that last 5–30 min, and in order to work in this time frame, manipulation of reaction rate is recommended (most routinely by increasing temperature or catalyst loading).

The PSI-ESI-MS methodology can be combined with any type of mass analyzer. When using a quadrupole time-of-flight (Q-TOF) spectrometer, precision to four decimal places is obtained, yielding accurate mass identification of analytes.<sup>[11,50–53]</sup> Triple quadrupole instruments provide a lower level of resolution; however, analyte identification can be confirmed through collision-induced dissociation whereby fragments are created from collisions with gas molecules. The resulting fragments can be used to create Multiple Reaction Monitoring (MRM) transitions effectively eliminating isobaric species, and analytes of interest can be observed in real time when coupled with PSI.<sup>[54]</sup> We demonstrated this method by monitoring the Buchwald-Hartwig amination reaction, where a charged ligand was used to track the catalytically relevant species of the reaction over time (Figure 3). Each component was added to the reaction flask sequentially to fully visualize each step in the catalytic cycle.

Cooks and coworkers have developed a pressurized system equipped with a specialized multi-sprayer source for sample delivery to a miniature mass spectrometer, which facilitates simultaneous reaction monitoring of several samples.<sup>[55]</sup> A stepper motor is used to rapidly switch between multiple spray emitters, with which they showed that cross contamination and interference was not an issue. Employing this system to monitor multiple hydrazone formation reactions yielded 6 h worth of data in just 2 h; however, more complex infrastructure is required to implement this system.

In-line derivatization can improve ionization of reaction components, and has been examined using PSI.<sup>[55]</sup> In this system, the reaction mixture was contained in one pressurized flask connected to a mixing tee piece. A second pressurized flask containing derivatization agent was connected to the other side of the tee piece, with the third inlet of the tee piece connected to the mass spectrometer. The reagents are allowed to interact in the mixing tee and immediate derivatization takes place. In this case, the derivatization procedure must be straight-forward without an incubation period. Additionally, the flow rate from each flask into the tee piece must be approximately equal to ensure proper mixing and flow into the mass spectrometer.

## 2.1. Detailed Experimental Setup

A Schlenk flask is placed close to the ESI source and is equipped with a rubber septum over the ground glass joint and a rubber hose on the arm. The rubber hose is connected to a regulated cylinder of  $\text{N}_2$  or other inert gas. The rubber septum is



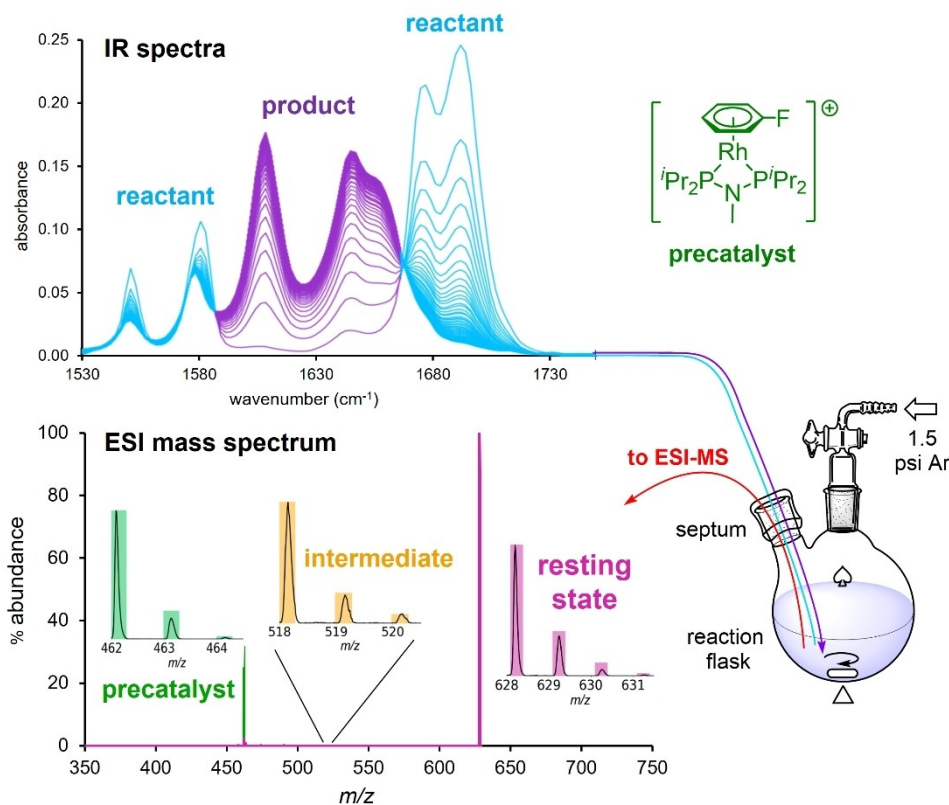


**Figure 2.** Combination of continuous monitoring methods to obtain IR and MS data for a hydroacylation reaction. From the same flask, tubing circulates the reaction solution through a flow FTIR spectrometer (top), and PEEK tubing exits into the mass spectrometer (bottom). Adapted with permission from Ref. [45]. Copyright 2016, American Chemical Society.

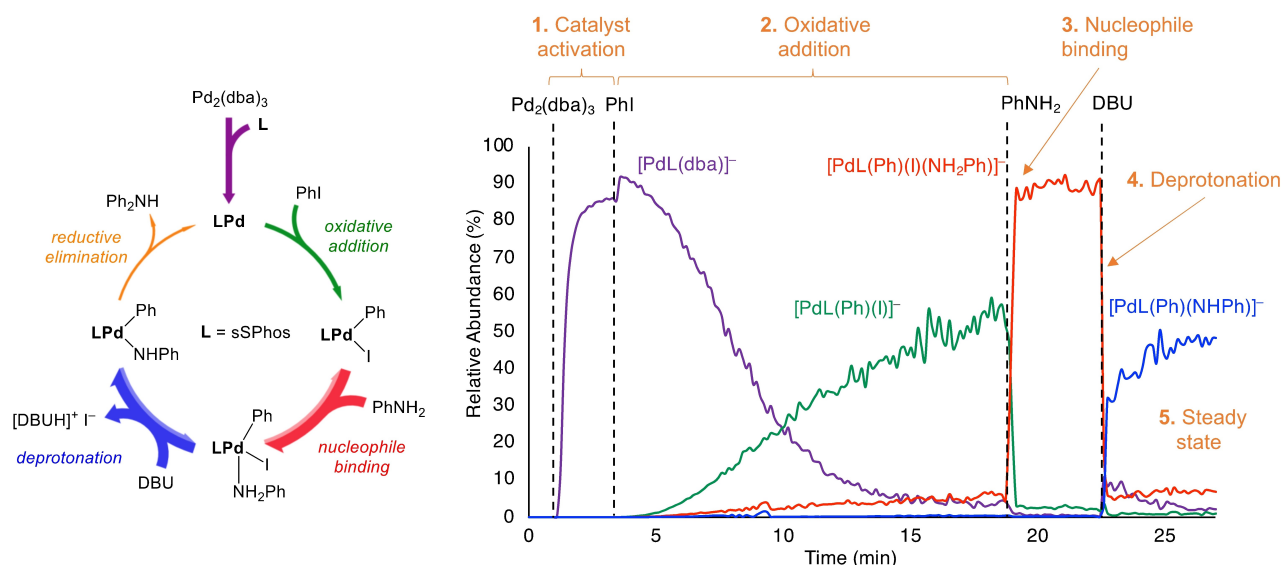


**Figure 3.** Catalytic cycle (left) and reaction monitoring trace (right) of a Buchwald-Hartwig amination reaction using MRM transitions. Dotted lines indicate sequential addition of reaction components. Reproduced with permission from Ref. [54]. Copyright 2019, Royal Society of Chemistry.

punctured with PEEK tubing extending into the reaction mixture, and the other end of the tubing is attached to the ESI source with a PEEK fitting (finger tight). If the septum is tough to puncture with the PEEK tubing, first puncture the septum using a needle approximately the same width as the outer

diameter of the tubing. After removing the needle, the PEEK tubing will fit through the hole in the septum. For heated reactions, a two-neck flask may be equipped with a condenser, or a specialized PSI flask with a built-in condenser may be used (Figure 4).<sup>[56]</sup> A stir bar may be placed into the flask with

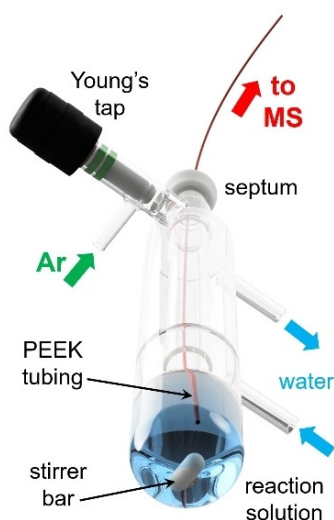


**Figure 4.** PSI flask equipped with condenser, adapted with permission from Ref. [56]. Copyright 2019, Elsevier.

reactants to ensure homogenous mixing. If reagents are not added to the flask inside a glovebox or on a Schlenk line, they are added through the rubber septum using a syringe. Beware: the positive pressure in the flask will force the syringe plunger away from the flask; this is prevented by holding a finger over the plunger while the needle is inside the flask. It is strongly recommended that the charged component of the reaction is added to the flask first, and the reaction initiated by adding neutral reactants. This precaution allows for optimization of ESI-MS conditions (spray quality, ion current) before the reaction is underway. See the Supporting Information for a video on how to set up a PSI experiment.

The reaction solution must flow through fittings with small internal diameters, so even though the PSI setup is simple, it is nonetheless vulnerable to plumbing issues. The inner diameter of the tubing, union and stainless-steel capillary are extremely small and can be easily blocked, especially if the reaction mixture is heterogeneous. If a blockage is present, a distinct spray pattern will present itself. The instrument will abruptly sense little to no ions, and then all of a sudden resume normal activity. This spray pattern may happen frequently or periodically depending on the severity of the blockage. When this occurs, simply disconnect the adapters and clean them before resuming the experiment as the data output will be inaccurate while a blockage is present. In severe cases where this mode of action does not rectify the issue, the capillary should be removed and sonicated in appropriate solvents. Blockages can be prevented by regular thorough cleaning/rinsing of these parts, use of filter material, and/or by using a homogeneous solution. Alternative methods of analyzing heterogeneous reaction mixtures have also recently been developed by Hein and coworkers.<sup>[57]</sup>

As in a cannula transfer, solutions may be filtered by securing filter material on the end of the tubing in the reaction flask. In such cases, the end of the capillary can be protected with (a suitably cut) filter paper, cotton wool, glass wool, or any

other filter material, and secured by use of Teflon tape. An example is illustrated in Figure 5. Here, standard filter papers (Watman, 55 Ø) are used with standard-density PTFE sealant tape to secure the filter paper to PEEK tubing as it does not interfere with the spectrum. The general steps for attaching the filters are shown, with the filter paper first cut into a T shape (Figure 5.2–3) and fit over the capillary opening. The stem of the paper is then folded over the capillary opening, with each arm then wrapping around the stem and capillary tube (Figure 5.4–6). A strip of PTFE tape is then used to secure the filter and seal the capillary tubing, which can be inserted into the reaction flask (Figure 5.7–9). It is important to avoid compromising flow rate or retention time, so using a minimal amount of filter material is desirable.

The effects of filtration on the PSI flow rate were tested, with the results illustrated in Figure 6. A PSI flask was set up as described in Figure 4; however, the end of the tubing that would be attached to the ESI source inlet was instead suspended above a flask that was placed on an analytical balance. The mass of solution flowing from the PEEK tubing was measured as a function of time, providing the PSI flow rate. A control trial with a homogeneous solution (THF) and no filtration (green) resulted in a consistent flow rate. In contrast, for a fine suspension (purple) ( $K_3PO_4$  in THF), the flow rate is seen to drastically drop after a minute of monitoring, indicating presence of a blockage. By attaching the filter described in Figure 5, clogging is effectively prevented.

Positioning of the tubing in the stirred solution can also have an effect on clogging issues, so placing it away from and above any circulating solid material is advised. For example, if the solid material is floating near the top of the reaction solution, place the PEEK tubing at the bottom of the flask. Decomposition of reaction components can often lead to the generation of precipitated material, and this problem can be consequential in terms of creating blockages. Reactions that produce solids, gels or polymeric material should be similarly approached with caution.

## 2.2. Interpretation of Time-Course Data

The resulting mass spectrum produced by PSI-ESI-MS is a reflection of how the ionic components of the reaction mixture change over time. The total ion chromatogram (TIC) is a sum of the abundance of all ions detected by the instrument over time. Extracted ion chromatograms (XIC) of each analyte displaying the abundance of a single ion over time can also be produced. The TIC always contains a certain amount of noise, as does the intensity versus time traces of individual ions, but the ratio between various ions is much more consistent than the absolute intensity. As such, each point in the chromatogram can be normalized to report the relative abundance of relevant reaction species (Figure 7). This is done by dividing the XIC intensity by the TIC intensity, and multiplying this quotient by 100 to obtain a percentage. These experiments are data dense in that each point in a chromatogram corresponds to its own mass spectrum. Scan times usually run on the order of

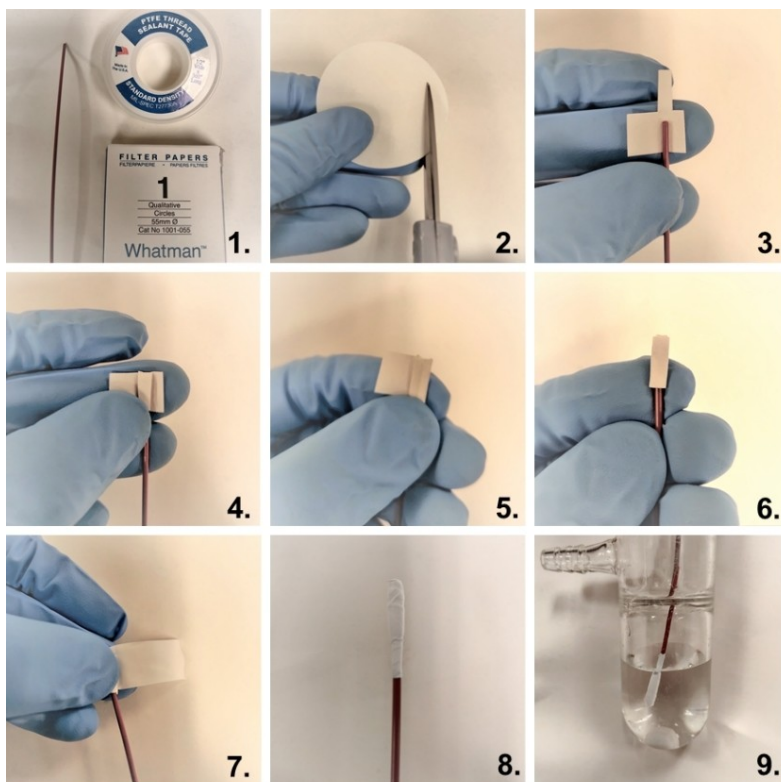


Figure 5. Preparation of paper filter for PSI PEEK tubing.

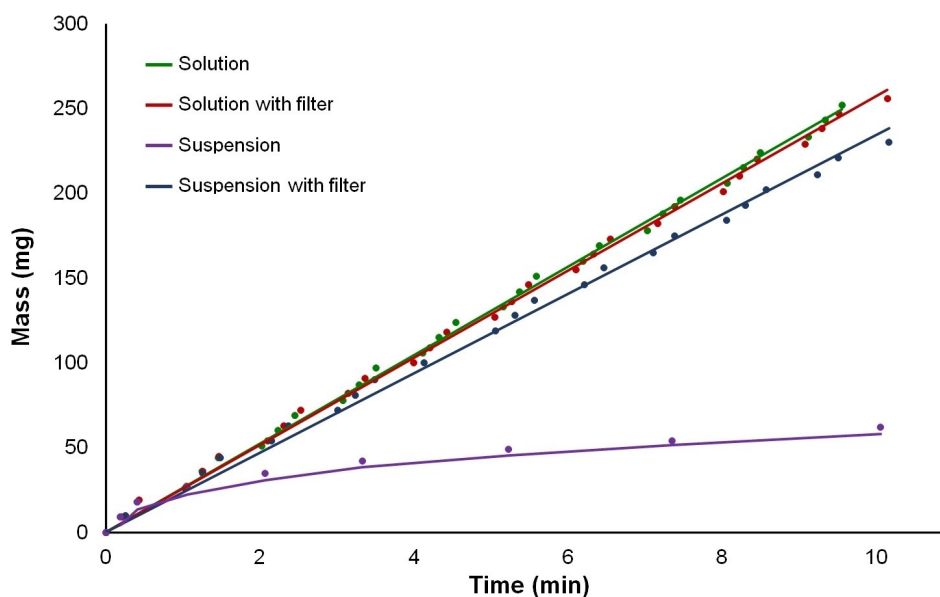
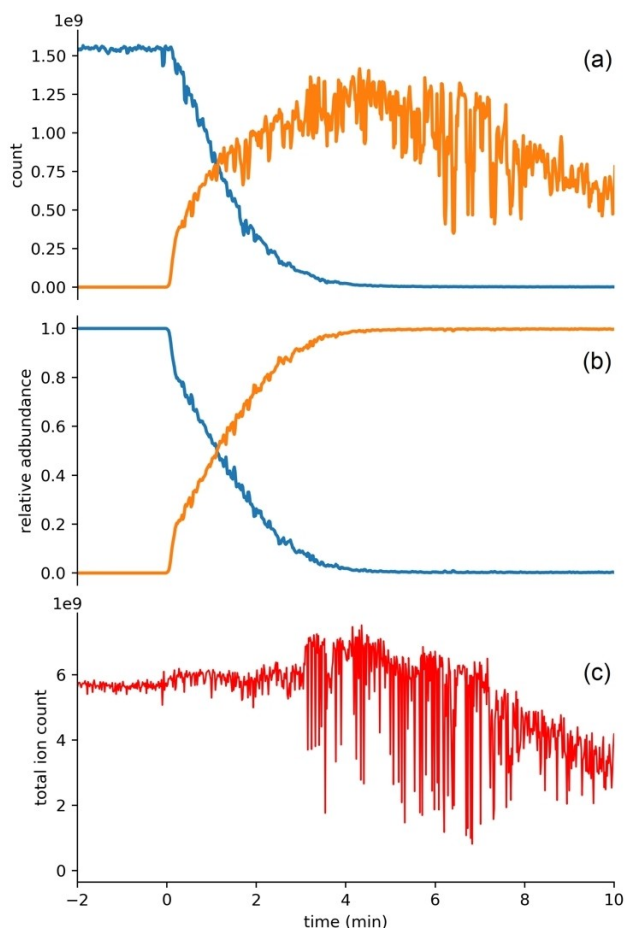


Figure 6. Mass of solution (mg) vs. time (min), illustrating the effect of attaching a filter to PEEK tubing in a heterogeneous reaction solution.

milliseconds, thus several spectra are being produced each second. After normalization, the calculated relative abundance of all species of interest can be plotted versus time. Spectra can be improved further by normalizing to the sum of all of the species of interest (thereby ignoring contributions from noise

and background ions). A variety of software is available to facilitate this process, including but not limited to PythoMS,<sup>[58]</sup> Origin, and Microsoft Excel.

Note the improvement in data quality upon normalization. This particular reaction is prone to decomposition of the excess



**Figure 7.** PSI-ESI-MS data depicting the effects of normalization. a) Extracted ion count vs. time data for a reaction between an alkyne and  $\text{Co}_2(\text{CO})_8$ ; b) Normalization of the data shown in (a); c) Total ion current (TIC) for the same reaction.

reagent  $\text{Co}_2(\text{CO})_8$  which produces the much less soluble  $\text{Co}_4(\text{CO})_{12}$  upon heating. It is this insoluble by-product that

causes the glitching in the TIC and the apparent decay in ion count. There are other reasons why the TIC may not be flat, including charge neutralization, generation of new charged species, or large changes in response factor of product compared to reactant. Checking the other ion mode is advisable in cases when the TIC shows strange behavior, because clues to the origin of that behavior can often be found there.

### 2.2.1. Normalization Precautions

Normalization obviously has a profound positive effect on the quality of the traces, but it is important to avoid applying it without consideration of the differential response factors of the ions of interest. ESI-MS does not exhibit one-to-one correspondence between peak intensity and concentration of a particular solution component, unlike NMR spectroscopy whereby the intensity of the peaks corresponds to the number of nuclei represented in each peak. The extent of ionization of a particular molecule is the most obvious contributor, but even in cases where two completely dissociated ions are compared, the surface activity of the ions can be markedly different. Ions which are strongly solvated will disproportionately occupy sites in the interior of the charged droplets produced during the electrospray ionization process, while larger hydrophobic ions preferentially migrate to the air-solvent interface on the surface of the droplets. As the droplet shrinks, charge density increases on the surface until the point that repulsion between like charges is sufficient to evaporate ions into the gas phase. A demonstration of this effect is seen in the comparison between  $\text{Cs}^+$  ( $m/z$  133) and a mixture of tetraalkylammonium ions, including  $[\text{NET}_4]^+$  ( $m/z$  130), wherein an ESI mass spectrum of a 1:1 mixture of the two will be overwhelmingly dominated by the quaternary ammonium ions (which themselves have different response factors) (Figure 8).<sup>[30]</sup>

In cases where the reactants and products are isolable, their relative response factors can be measured easily, and the data

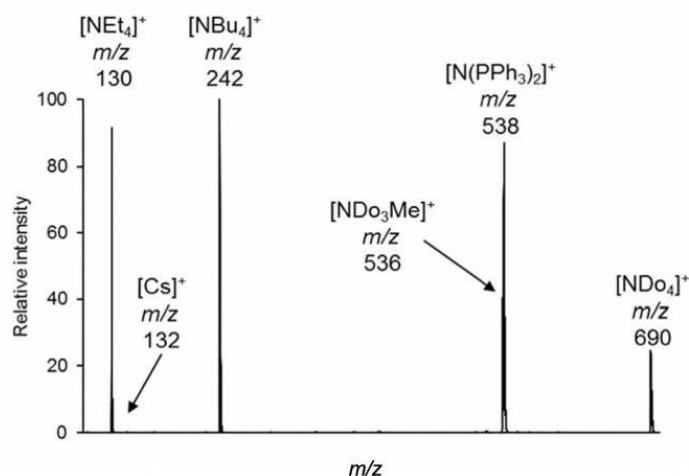


**Figure 8.** Positive ion ESI mass spectrum of an equimolar mixture of six cations  $[\text{NET}_4]^+$  ( $m/z$  130),  $[\text{Cs}]^+$  ( $m/z$  132),  $[\text{NBu}_4]^+$  ( $m/z$  242),  $[\text{N}(\text{PPh}_3)_2]^+$  ( $m/z$  538),  $[\text{NDO}_3\text{Me}]^+$  ( $m/z$  536), and  $[\text{NDO}_4]^+$  ( $m/z$  690), with  $\text{Cl}^-$  counterion in acetonitrile (Do = dodecyl). Adapted with permission from Ref. [30]. Copyright 2019, American Society for Mass Spectrometry.



accordingly corrected. For example, if the product has a response factor  $2/3$  of the reactant, the intensity of that ion should be multiplied by  $3/2$  for the entire trace. This sort of data treatment is analogous to what is done in UV-Vis spectroscopy, for example, where the extinction coefficient of different analytes can be very different. Not applying such corrections will have distorting effects on the traces, can affect the linearity of the plots used to determine rate constants and/or affect the values of those rate constants, and in extreme cases can lead to wrong-headed interpretations of the chemistry. These distortions are best illustrated by use of figures, and we have plotted in Figure 9 the effect of different

response factors on plots for 0<sup>th</sup>, 1<sup>st</sup> and 2<sup>nd</sup> order chemical reactions. The Supporting Information contains animations of the noisy total ion current (TIC, top right), the linear plot establishing the rate constant (middle right, not included for zero order as the main graph performs that task), the noisy raw data (bottom right), and the normalized data (main plot, left), where the response factor of the product ranges from  $0.1 \times$  to  $10 \times$  that of the reactant. The snapshots in Figure 9 were chosen to show how normalizing the data from zeroth, first and second order reactions can all look similar if the response factors are not taken into account.

Note that while the raw data is noisy, it contains a lot of information about the relative response factors itself. Assuming a 100% conversion of A (reactant) to B (product), the relative proportions at the crossing point are the same as the response factor ratio, as is the relative ratio of A at the starting point to B at the completion of the reaction. However, this sort of perfectly clean reaction is far from the norm, and so direct measurements of relative response factors are advised where accurate rate constants are required.

We have also provided in the Supporting Information a spreadsheet that allows visualization of the effect of normalization for any response factor for the three different orders of reaction, and animations showing the various possibilities. Some distortions are predictable, but others less so, such as the fact that, for a second order reaction, any plot of  $1/[x]$  versus time generates a straight line after normalization, regardless of the response factor.

One encouraging observation is that, provided response factors are reasonably close to one another (and related ions often are), the amount of error is fairly small. It is often the case that relative response factors are NOT directly measurable because the species of interest is short-lived (e.g. a reactive intermediate, a product of limited stability, a resting state stable only in the presence of substrate and/or product, etc.). If we are looking at a set of similar ions, for example cationic complexes with a common ancillary ligand set, the surface activity of that set of ions is likely to be close to each other, and the approximation that these species share the same response factor is a reasonable one. This approximation is particularly good when the TIC remains fairly constant over the course of a reaction, since such an observation suggests good mass balance. A TIC that grows or decays in a way related to the overall progress of the reaction is a sign that the mass balance is poor. Note that, however, there are other reasons why the TIC may vary during a PSI experiment – for example accumulation of debris in the tubing can cause slow choking of the flow rate and hence ion count, (as previously mentioned). As is the case with any experiment, replicates greatly increase confidence in results.

### 2.2.2. Saturation

The sensitivity of ESI-MS can be a double-edged sword: it is fantastic for measuring low abundance species, but it is poorly suited to handle high or even moderate concentrations of

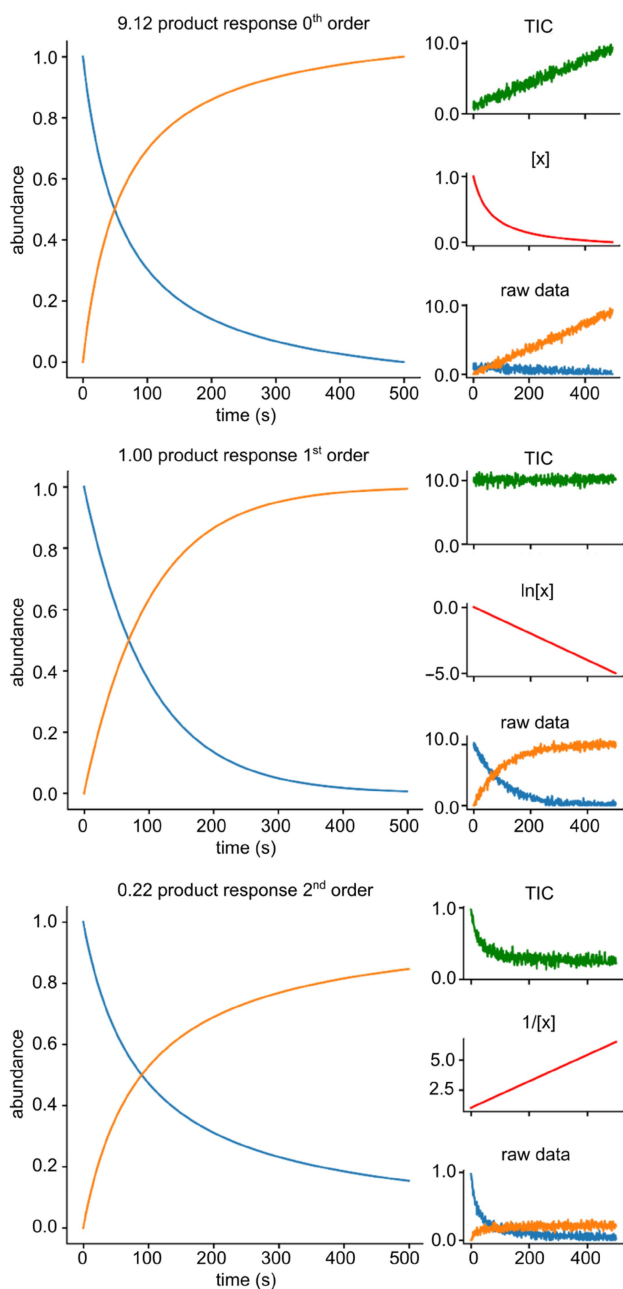


**Figure 9.** Normalized data for zeroth, first and second order reactions where product to starting material response factor is 9.12:1, 1:1 and 0.22:1, respectively. More data available in the Supporting Information.

molecules that easily ionize (or permanently charged ions). Saturation distorts spectra by reducing the apparent intensity of the most abundant ions, and there are a number of clues that saturation is occurring. Individual peak shapes are often distorted (square-topped peaks, broad peaks) and isotope patterns often provide poor matches to calculated patterns. The fact that saturation affects peaks of different intensities in different ways offers a quick check of whether saturation is occurring or not: simply generate a time course profile for one of the smaller peaks in the isotope pattern, and see if it changes shape (it will inevitably have a lower signal-to-noise ratio).<sup>[59]</sup> Figure 10 depicts a reaction profile whereby the reagent saturates the spectrum. It is clear that the M and M + 1 traces differ from one another, and the M + 2 is similar to the M + 1 trace, though, predictably, it has a lower signal-to-noise ratio.

In terms of mitigating saturation, it is not always as easy as “make the solution more dilute”. This precaution can slow the reaction down to the point where it is no longer examinable on a desirable time scale or, even more problematically, increased decomposition takes place at low concentration. There are also often limits to how much the reaction can be accelerated in

compensation for lower concentration by heating and/or increasing catalyst loading. ESI-MS is sufficiently sensitive that it is relatively easy to detect analytes at concentration levels similar to the amount of residual oxygen and moisture present in even carefully dried solvent ( $\approx 5$  ppm). Expecting good results when reactive contaminants are present at stoichiometric levels is not realistic, so high concentrations are often employed simply to reduce the proportion of decomposition observed. As such, saturation is a problem often encountered by the chemist working on air- and moisture-sensitive materials. Detuning instrument sensitivity by a variety of different methods (reducing capillary voltage to lower the amount of excess charge created, increasing the flow of cone gas to blow away ions from entering the mass spectrometer, increasing capillary to cone distance, damping the detector sensitivity) may be necessary.<sup>[60]</sup> This sort of trade-off (avoiding saturation vs. decomposition) has to be done carefully while checking that the relative response to different ions is not significantly perturbed.<sup>[30,61]</sup>

### 3. Applications

#### 3.1. Applications in Organic Reaction Monitoring

A [3 + 2] cycloaddition/oxidation/aromatization reaction responsible for synthesis of bioactive pyrrolo[2,1-a]isoquinolines and indolizino[8,7-b]indoles was studied continuously for 6 h using the PSI-ESI-MS method to elucidate the mechanistic intermediates in the reaction where a green catalytic system (tetrabutylammonium iodide (TBAI)/*tert*-butyl hydroperoxide (TBHP)) was used in the reaction.<sup>[62]</sup> In this case, a charged-tag was not needed as the zwitterionic intermediates were in equilibrium with their protonated form. The intermediates of the environmentally friendly reaction were successfully monitored and characterized using PSI-ESI-MS/MS.

A Ritter-type reaction involving menthol,  $\text{CuBr}_2$ ,  $\text{Zn}(\text{OTf})_2$ , Selectfluor®, and acetonitrile resulting in C–H amination of secondary and tertiary C–H bonds was reported in 2012 by Baran et al.,<sup>[63]</sup> and studied in real-time by Zare et al. in 2018.<sup>[64]</sup> The PSI-ESI-MS technique facilitated the proposal of a more thorough mechanism by observation of several reaction intermediates, and exposed two mechanistic pathways whereby one pathway occurs in bulk solution and the other pathway occurs in microdroplets. The microdroplets created in ESI-MS allow for  $\text{H}^+$  to accumulate on the surface of the droplet, thereby promoting acid-catalyzed reactions despite the absence of acid, and such conditions are required to create the intermediate observed in the microdroplet mechanism. (Figure 11).

Vicent and Gusev's 2016 study of acceptorless dehydrogenative coupling (ADC) of alcohols sings praise for the PSI technique stating that “[PSI] has proved to be ideal for in situ analysis of complex mixtures formed during catalysis”.<sup>[65]</sup> Their research highlighted several intermediates in the reaction, and used CID to facilitate structure elucidation in combination with isotope patterns.

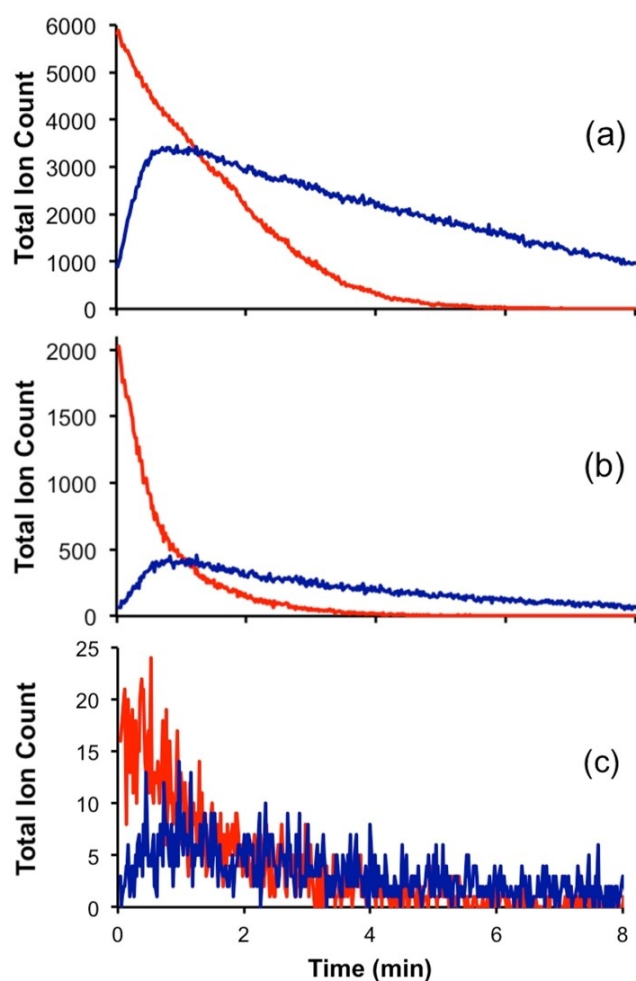


**Figure 10.** Representative saturation PSI-ESI-MS traces for (a) M, (b) M + 1 and (c) M + 2. The red trace is the reagent, and the blue trace is one of the products. Adapted with permission from Ref. [60]. Copyright 2020, Elsevier.

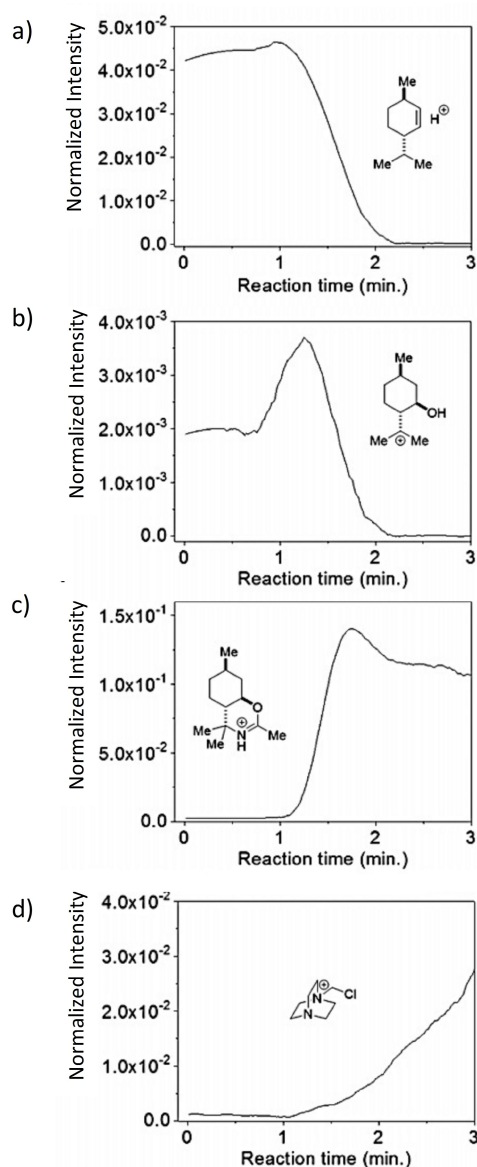


**Figure 11.** PSI-ESI-MS monitoring of a C–H amination reaction using  $\text{CuBr}_2$ ,  $\text{Zn}(\text{OTf})_2$ , and Selectfluor in acetonitrile. a) Starting material; b) Cationic intermediate; c) Product; d) Reduced Selectfluor<sup>®</sup> by-product. Adapted with permission from Ref. [64]. Copyright 2018, American Chemical Society.

### 3.2. Applications in Catalysis

Mechanistic analysis has long been of significant interest in the community, and PSI-ESI-MS has been an extremely useful tool in uncovering reaction intermediates<sup>[47,66–70]</sup> as well as kinetic profiles.<sup>[71–73]</sup> Several examples are described here.

Mack et al. discovered the degradation mechanism of their  $[(\text{dtbpy})_2\text{Ru}(\text{CO}_3)]$  ( $\text{dtbpy}$  = 4,4'-di-*tert*-butyl-2,2'-bipyridine) pre-catalyst using PSI-ESI-MS.<sup>[74]</sup> It was discovered that the catalyst activity can be inhibited by dimerization and ligand dissociation. Upon further PSI-ESI-MS probing, it was determined that catalyst dimerization only played a minor role in inhibition, and that ligand dissociation was mostly responsible for limiting

turnover. The authors were also able to elucidate the mechanism of this ligand dissociation process.

McIndoe and coworkers investigated the Suzuki-Miyaura reaction in positive and negative ion mode using charge-tags to ensure observation of each intermediate.<sup>[75]</sup> Their results indicate that at least two mechanisms are at work in the reaction. Further mechanistic work was done by the same group on the Pauson-Khand reaction involving the  $\text{Co}_2(\text{CO})_8$  catalyst as well as a charged alkene to track the progress of both intermolecular and intramolecular reactions.<sup>[76]</sup> The rate-determining step in the reaction was revealed to be CO dissociation, and it was concluded that the nature of the alkene does not play a role in catalyst coordination.

The Newman group's investigation of chemoselectivity in the Kumada-Corriu cross-coupling reaction employed PSI-ESI-MS to determine the mechanism of the reaction during slow addition of  $\text{PhMgBr}$  (Figure 12).<sup>[77]</sup> The catalytic cycle consists of oxidative addition, transmetalation of  $\text{PhMgBr}$ , and reductive elimination. If the Grignard reagent is added faster than the oxidative addition product ( $\text{ArPdCl}$ ) is formed, the reactive  $\text{PhMgBr}$  will quench the excess aryl halide and create side products. During real-time analysis, the concentration of side products was significantly decreased when the Grignard reagent was added slowly over the course of 1 h, versus a faster 5 min addition. It was concluded that the oxidative addition product must be present to prevent the  $\text{PhMgBr}$  from reacting with another species, and as a result the yield of desired product was increased.

A mechanistic examination of the copper-mediated conversion of arylboronate esters into aryl fluorides was conducted by Hartwig and co-workers.<sup>[78]</sup> In this case, PSI-ESI-MS facilitated identification of a copper(III) fluoride product in solution as it was not isolatable.

An eco-friendly catalyst system of tetrabutylammonium iodide/*tert*-butyl hydroperoxide was explored in forming pyrrolo[2,1-*a*]isoquinolines and indolizino[8,7-*b*]indoles, both

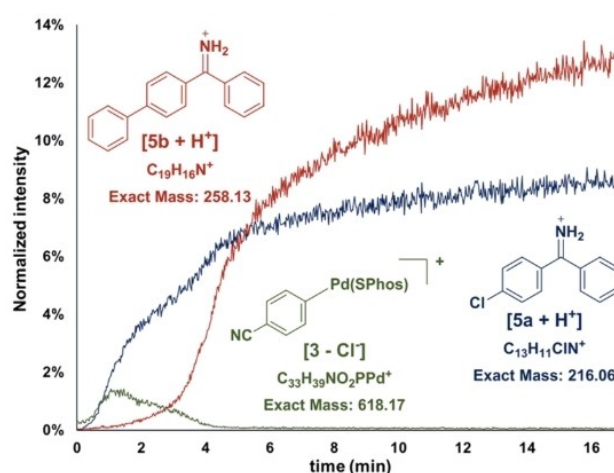


**Figure 12.** Real-time PSI-ESI-MS analysis of the Kumada-Corriu cross-coupling between  $\text{PhMgBr}$  and chlorobenzonitrile with fast addition of  $\text{PhMgBr}$ . Adapted with permission from Ref. [78]. Copyright 2016, American Chemical Society.

products holding pharmaceutical significance.<sup>[62]</sup> The intermediates involved in the [3 + 2] cycloaddition/oxidation/aromatization cascade reaction were identified for the first time using the PSI-ESI-MS technique. The identity of key intermediates was confirmed using ESI-MS/MS.

Alcohol oxidation, oxygen activation, and H<sub>2</sub>O<sub>2</sub> disproportionation reactions were examined in real time using PSI by Waymouth and coworkers (Figure 13).<sup>[79]</sup> Combined with isotope-labeling and kinetic studies, key reaction intermediates were identified in reaction mechanisms occurring simultaneously – some multinuclear! The study opened up new avenues for exploration of oxygenation chemistry with palladium.

A look into palladium/diene-catalyzed coupling of alkyl halides and Grignard reagents revealed that anionic Pd complexes are formed, and the mononuclear species are short-lived – mainly favouring formation of small Pd nanoclusters.<sup>[80]</sup> The real-time MS analysis afforded direct aggregation state information as well. Additionally, the study discovered that the transmetalation step in these reactions actually precedes the oxidative addition step in the catalytic cycle.

PSI-ESI-MS has also proven useful for Belli et al. in comparing the affinity of select secondary and tertiary phosphines for cationic ruthenium centers.<sup>[81]</sup> Competitive substitution reactions were analyzed in real time to assess the relative binding strength and measure the relative kinetics. A dissociative mechanism for substitution of NCPH with secondary phosphines on [Ru( $\eta^5$ -indenyl)(NCPH)(PPh<sub>3</sub>)<sub>2</sub>]<sup>+</sup> was revealed, as well as reaction kinetics. When comparing steric and electronic effects, the authors discovered that steric hinderance of the secondary phosphine plays a prominent role. In contrast, tertiary phosphines were found to produce multiple products as the Ru–PPh<sub>3</sub> bonds are weakened upon substitution of NCPH with P(<sup>n</sup>Bu)<sub>3</sub>. Ramping the collision energy revealed the relative binding strength of three ligands: PEt<sub>2</sub>H > PPh<sub>2</sub>H ≈ PPh<sub>3</sub>. These experiments were conducted in tandem with <sup>31</sup>P{<sup>1</sup>H} NMR spectroscopic studies which corroborated the ESI-MS results (Figure 14). These data also nicely illustrate the difference in typical concentration range between the two techniques,<sup>[82,83]</sup>

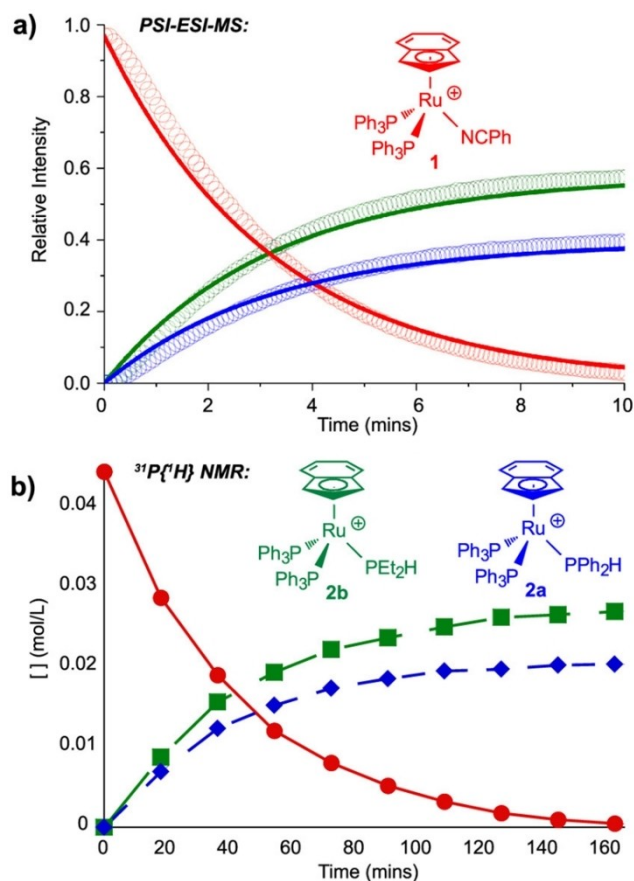


**Figure 14.** (a) Competitive reactions of [Ru( $\eta^5$ -indenyl)(NCPH)(PPh<sub>3</sub>)<sub>2</sub>]<sup>+</sup> with a 10:10 mixture of PPh<sub>2</sub>H/PEt<sub>2</sub>H at 45 °C in fluorobenzene, as monitored by PSI-ESI-MS. Circles are normalized experimental data; lines are simulated using parameter estimation with COPASI. (b) 145.85 MHz <sup>31</sup>P{<sup>1</sup>H} NMR data for the same experiment in 2:1 CH<sub>2</sub>Cl<sub>2</sub>/C<sub>6</sub>D<sub>6</sub> at RT. Adapted with permission from Ref. [82]. Copyright 2019, American Chemical Society.

with the NMR spectroscopy studies being conducted at three million times higher concentration than the ESI-MS in this case.

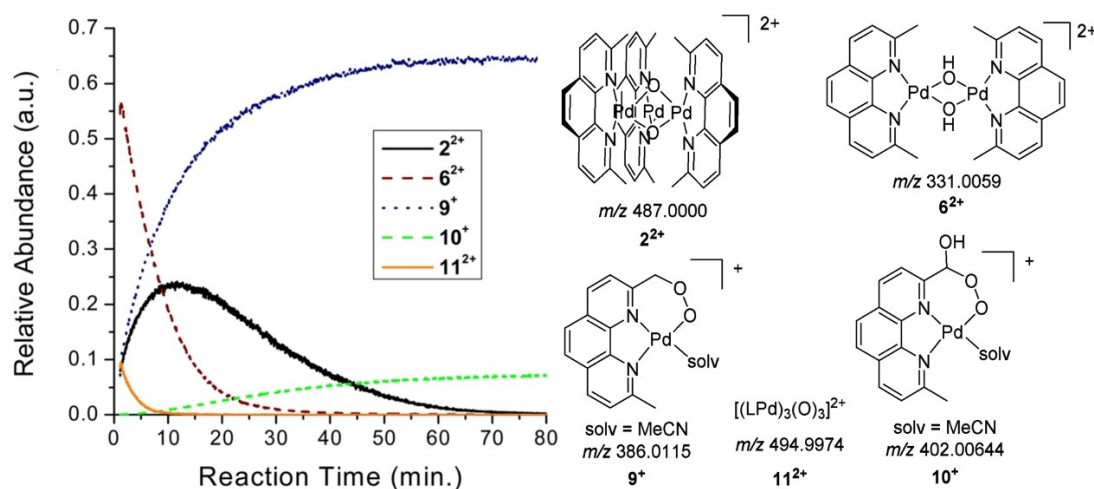


**Figure 13.** Left: PSI-ESI-MS monitoring of an H<sub>2</sub>O<sub>2</sub> disproportionation reaction with [(LPd(OAc))(OTf)<sub>2</sub>] (L = 2,9-dimethyl-1,10-phenanthroline). Right: proposed structures of speciation. Adapted with permission from Ref. [80]. Copyright 2015, American Chemical Society.



The capabilities of PSI-ESI-MS can shed light on ‘simple’ reaction systems as well. For example, titanocene has been used as an indicator of oxidation and the presence of O<sub>2</sub>. In what was previously known as a straightforward reaction, Cp<sub>2</sub>Ti<sup>IV</sup>X<sub>2</sub> was reduced to Ti<sup>III</sup> followed by oxidation back to Ti<sup>IV</sup>. In acetonitrile, the oxidized species, [Cp<sub>2</sub>Ti(NCMe)<sub>2</sub>]<sup>2+</sup>, is yellow in colour. Real-time analysis has revealed that the oxidation is not as simple as it seems. In fact, a variety of oxygen-containing products were generated, and [Cp<sub>2</sub>Ti(NCMe)<sub>2</sub>]<sup>2+</sup> was found to be quite reactive toward protic solvents.<sup>[84]</sup> When the reaction was tested in the presence of water, it was found that the oxidation proceeded slowly and required a significant amount of water, making this system non-ideal for detection of trace amounts of water in reactions and gloveboxes alike.

The PSI technique is also capable of handling extremely air- and moisture-sensitive systems such as olefin polymerization catalysts (Figure 15).<sup>[85]</sup> The reaction shown is that between [Cp<sub>2</sub>ZrMe<sub>2</sub>AlMe<sub>2</sub>][B(C<sub>6</sub>F<sub>5</sub>)<sub>4</sub>] and (a) 100 and (b) 1000 equivalents of hexene, a reaction that results in polymerization of the hexene and a range of decomposition pathways for the catalyst precursor. Note the ability of the technique to provide reaction

rates and identification of the various catalyst deactivation products.

## 4. Summary and Outlook

PSI-ESI-MS has strong capabilities in reaction monitoring and observation of reaction intermediates under air- and moisture-free conditions. The method has been described as a “break-through strategy” in terms of online acquisition of high-quality data.<sup>[86]</sup> The low pressure system, driving the solution through a small diameter capillary, can lead to obstruction of the flow path, a phenomenon less prominent in high pressure systems. This issue can be problematic at times due to the influence on the resulting kinetic profile, especially in heterogeneous systems which are more prone to clogging and require dynamic mixing systems. PSI-ESI-MS is also not compatible with concentrations at the process level, so innovating a way of doing so is an important next step for this technique. Despite these challenges, the speed, ability to cope with complex mixtures, and extremely high sensitivity of mass spectrometry is superior to several other analytical techniques, and a robust sample delivery system is a critical tool to build and extend its applications.

## Supporting Information

A flow rate calculator, video illustration of the PSI-ESI-MS set-up, and animations illustrating the effect of normalization on kinetic traces depending on relative response factors are contained in the Supporting Information of this article.

## Acknowledgements

J. S. M. thanks the NSERC Discovery program for operational funding and CFI, BCKDF and the University of Victoria for infrastructural support. Thanks to all of the students who developed and refined the PSI technique over the years, especially Krista Kobylanskii, Zohrab Ahmadi, Jingwei Luo, Rhonda Stoddard, Lars Yunker, Eric Janusson, Robin Theron, Anuj Joshi, and Isaac Omari.

## Conflict of Interest

The authors declare no conflict of interest.

**Keywords:** mass spectrometry · on-line monitoring · pressurized sample infusion · reaction mechanisms · real-time monitoring

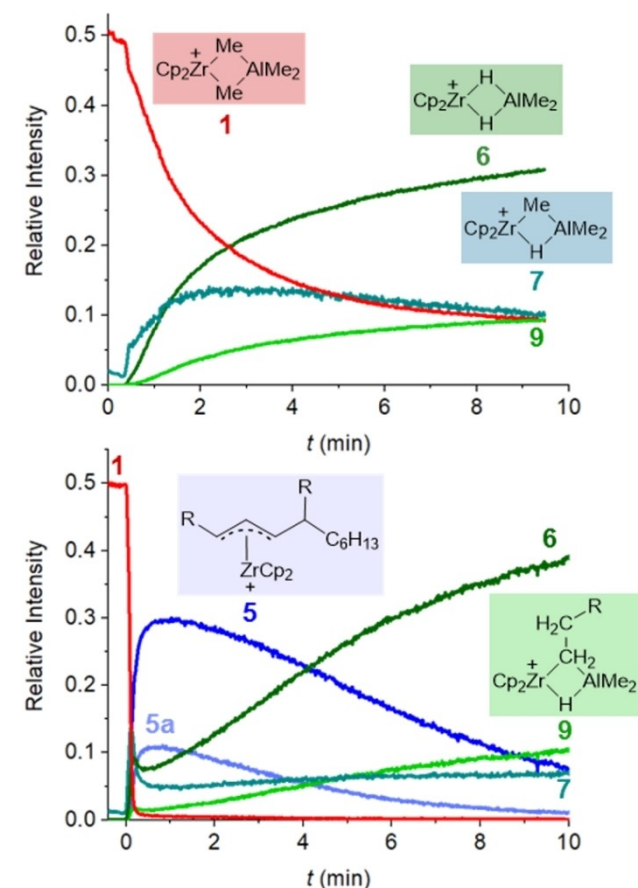


**Figure 15.** Normalized ion intensities vs. time for addition of (top) 100 equivalents, and (bottom) 1000 equivalents of hexene to [Cp<sub>2</sub>ZrMe<sub>2</sub>AlMe<sub>2</sub>][B(C<sub>6</sub>F<sub>5</sub>)<sub>4</sub>] in difluorobenzene solution with [Zr] = 0.28 mM; R = “Bu”. Adapted with permission from Ref. [86]. Copyright 2020, American Chemical Society.

[1] S. Görög, *TrAC Trends Anal. Chem.* **2007**, *26*, 12–17.

[2] T. C. Malig, J. D. B. Koenig, H. Situ, N. K. Chehal, P. G. Hultin, J. E. Hein, *React. Chem. Eng.* **2017**, *2*, 309–314.

- [3] T. C. Malig, L. P. E. Yunker, S. Steiner, J. E. Hein, *ACS Catal.* **2020**, *10*, 13236–13244.
- [4] T. Maschmeyer, P. L. Prieto, S. Grunert, J. E. Hein, *Magn. Reson. Chem.* **2020**, *58*, 1234–1248.
- [5] M. Khajeh, M. A. Bernstein, G. A. Morris, *Magn. Reson. Chem.* **2010**, *48*, 516–522.
- [6] C. P. Johnston, T. H. West, R. E. Dooley, M. Reid, A. B. Jones, E. J. King, A. G. Leach, G. C. Lloyd-Jones, *J. Am. Chem. Soc.* **2018**, *140*, 11112–11124.
- [7] A. García-Domínguez, P. H. Helou De Oliveira, G. T. Thomas, A. R. Sugranyes, G. C. Lloyd-Jones, *ACS Catal.* **2021**, *11*, 3017–3025.
- [8] R. Wei, A. M. R. Hall, R. Behrens, M. S. Pritchard, E. J. King, G. C. Lloyd-Jones, *Eur. J. Org. Chem.* **2021**, 2021, 2331–2342.
- [9] B. Gouilleux, B. Charrier, S. Akoka, P. Giraudeau, *Magn. Reson. Chem.* **2017**, *55*, 91–98.
- [10] W. Henderson, J. S. McIndoe, *Mass Spectrometry of Inorganic, Coordination and Organometallic Compounds: Tools - Techniques - Tips*, John Wiley & Sons, Ltd, West Sussex, **2005**.
- [11] J. H. Gross, *Mass Spectrometry*, Springer International Publishing, Cham, **2017**.
- [12] I. Bertini, C. Luchinat, G. Parigi, E. Ravera, *NMR of Paramagnetic Molecules: Applications to Metallobiomolecules and Models, Volume 2*, Elsevier, Amsterdam, **2017**.
- [13] M. C. McMaster, *LC/MS: A Practical User's Guide*, John Wiley & Sons, Hoboken, **2005**.
- [14] B. Boyd, R. K. Boyd, C. Basic, R. Bethem, *Trace Quantitative Analysis by Mass Spectrometry*, John Wiley & Sons, Chichester, **2008**.
- [15] L. S. Santos, *Eur. J. Org. Chem.* **2008**, 2008, 235–253.
- [16] L. S. Santos, *Reactive Intermediates: MS Investigations in Solution*, Wiley-VCH, Weinheim, **2010**.
- [17] K. L. Johnson, T. D. Veenstra, J. M. Londowski, A. J. Tomlinson, R. Kumar, S. Naylor, *Biomed. Chromatogr.* **1999**, *13*, 37–45.
- [18] D. J. Orton, M. M. Tfaily, R. J. Moore, B. L. LaMarche, X. Zheng, T. L. Fillmore, R. K. Chu, K. K. Weitz, M. E. Monroe, R. T. Kelly, R. D. Smith, E. S. Baker, *Anal. Chem.* **2018**, *90*, 737–744.
- [19] A. Bjarnason, R. E. DesEnfants II, M. E. Barr, L. F. Dahl, *Organometallics* **1990**, *9*, 657–661.
- [20] R. L. Stoddard, S. Collins, J. S. McIndoe, in *PATAI's Chem. Funct. Groups (Ed.: Z. Rappoport)*, **2016**, pp. 1–15.
- [21] J. Penafiel, A. V. Hesketh, O. Granot, J. S. McIndoe, *Dalton Trans.* **2016**, 45, 15552–15556.
- [22] M. D. Eelman, J. M. Blacquiere, M. M. Moriarty, D. E. Fogg, *Angew. Chem. Int. Ed.* **2008**, *47*, 303–306; *Angew. Chem.* **2008**, *120*, 309–312.
- [23] A. T. Lubben, J. S. McIndoe, A. S. Weller, *Organometallics* **2008**, *27*, 3303–3306.
- [24] K. L. Vikse, M. P. Woods, J. S. McIndoe, *Organometallics* **2010**, *29*, 6615.
- [25] R. J. Errington, *Advanced Practical Inorganic and Metalorganic Chemistry*, Chapman & Hall, London, **1997**.
- [26] K. L. Vikse, Z. Ahmadi, J. S. McIndoe, *Coord. Chem. Rev.* **2014**, *279*, 96–114.
- [27] K. L. Vikse, Z. Ahmadi, C. C. Manning, D. A. Harrington, J. S. McIndoe, *Angew. Chem. Int. Ed.* **2011**, *50*, 8304–8306; *Angew. Chem.* **2011**, *123*, 8454–8456.
- [28] H. Zhu, E. Janusson, J. Luo, J. Piers, F. Islam, G. B. Mcgarvey, A. G. Oliver, O. Granot, J. S. McIndoe, *Analyst* **2017**, *142*, 3728–3284.
- [29] U. Gellrich, A. Meißner, A. Steffani, M. Kähny, H. J. Drexler, D. Heller, D. A. Plattner, B. Breit, *J. Am. Chem. Soc.* **2014**, *136*, 1097–1104.
- [30] I. Omari, P. Randhawa, J. Randhawa, J. Yu, J. S. McIndoe, *J. Am. Soc. Mass Spectrom.* **2019**, *30*, 1750–1757.
- [31] W. Henderson, C. Evans, *Inorg. Chim. Acta* **1999**, *294*, 183–192.
- [32] L. S. Santos, G. B. Rosso, R. A. Pilli, M. N. Eberlin, *J. Org. Chem.* **2007**, *72*, 5809–5812.
- [33] N. J. Farrer, R. McDonald, J. S. McIndoe, *Dalton Trans.* **2006**, 4570–4579.
- [34] N. J. Farrer, R. McDonald, T. Piga, J. S. McIndoe, *Polyhedron* **2010**, *29*, 254–261.
- [35] W. Henderson, B. K. Nicholson, *J. Chem. Soc. Chem. Commun.* **1995**, 2531–2532.
- [36] C. Decker, W. Henderson, B. K. Nicholson, *J. Chem. Soc. Dalton Trans.* **1999**, 3507–3513.
- [37] C. Hinderling, C. Adlhart, P. Chen, *Angew. Chem. Int. Ed.* **1998**, *37*, 2685–2689; *Angew. Chem.* **1998**, *110*, 2831–2835.
- [38] D. M. Chisholm, A. G. Oliver, J. S. McIndoe, *Dalton Trans.* **2010**, 39, 364–373.
- [39] C. Adlhart, P. Chen, *Helv. Chim. Acta* **2000**, *83*, 2192–2196.
- [40] E. Crawford, T. Lohr, E. M. Leitao, S. Kwok, J. S. McIndoe, *Dalton Trans.* **2009**, 9110–9112.
- [41] A. Mesias-Salazar, O. S. Trofymchuk, C. G. Daniliuc, A. Antiñolo, F. Carrillo-Hermosilla, F. M. Nachtigall, L. S. Santos, R. S. Rojas, *J. Catal.* **2020**, *382*, 150–154.
- [42] M. Kumar, S. Verma, A. Kumar, P. K. Mishra, R. O. Ramabhadran, S. Banerjee, A. K. Verma, *Chem. Commun.* **2019**, 55, 9359–9362.
- [43] M. A. Henderson, J. S. McIndoe, *Chem. Commun.* **2006**, 2872–2874.
- [44] A. V. Hesketh, S. Nowicki, K. Baxter, R. L. Stoddard, J. S. McIndoe, *Organometallics* **2015**, *34*, 3816–3819.
- [45] R. Theron, Y. Wu, L. P. E. Yunker, A. V. Hesketh, I. Pernik, A. S. Weller, J. S. McIndoe, *ACS Catal.* **2016**, *6*, 6911–6917.
- [46] G.-J. Cheng, X.-M. Zhong, Y.-D. Wu, X. Zhang, *Chem. Commun.* **2019**, 55, 12749–12764.
- [47] A. Y. Kostyukovich, A. M. Tsedilin, E. D. Sushchenko, D. B. Eremin, A. S. Kashin, M. A. Topchiy, A. F. Asachenko, M. S. Nechaev, V. P. Ananikov, *Inorg. Front.* **2019**, *6*, 482–492.
- [48] S. P. Sutura, R. Skalac, *Annu. Rev. Fluid Mech.* **1993**, *25*, 1–20.
- [49] K. L. Vikse, Z. Ahmadi, J. Luo, N. Van Der Wal, K. Daze, N. Taylor, J. S. McIndoe, *Int. J. Mass Spectrom.* **2012**, *323*, 8–13.
- [50] S. A. McLuckey, J. M. Wells, *Chem. Rev.* **2001**, *101*, 571–606.
- [51] M. Guilhaus, D. Selby, V. Mlynski, *Mass Spectrom. Rev.* **2000**, *19*, 65–107.
- [52] I. V. Chernushevich, A. V. Loboda, B. A. Thomson, *J. Mass Spectrom.* **2001**, *36*, 849–865.
- [53] A. L. Burlingame, R. K. Boyd, S. J. Gaskell, *Anal. Chem.* **1994**, *66*, 634–683.
- [54] G. T. Thomas, E. Janusson, H. S. Zijlstra, J. S. McIndoe, *Chem. Commun.* **2019**, 55, 11727–11730.
- [55] C. J. Pulliam, R. M. Bain, H. L. Osswald, D. T. Snyder, P. W. Fedick, S. T. Ayrton, T. G. Flick, R. G. Cooks, *Anal. Chem.* **2017**, *89*, 6969–6975.
- [56] G. T. Thomas, L. MacGillivray, N. L. Dean, R. L. Stoddard, L. P. E. Yunker, J. S. McIndoe, *Int. J. Mass Spectrom.* **2019**, *441*, 14–18.
- [57] Y. Sato, J. Liu, A. J. Kukor, J. C. Culhane, J. L. Tucker, D. J. Kucera, B. M. Cochran, J. E. Hein, *J. Org. Chem.* **2021**, *86*, 14069–14078.
- [58] L. P. E. Yunker, S. Donneck, M. Ting, D. Yeung, J. S. McIndoe, *J. Chem. Inf. Model.* **2019**, *59*, 1295–1300.
- [59] A. Bilbao, B. C. Gibbons, G. W. Slysz, K. L. Crowell, M. E. Monroe, Y. M. Ibrahim, R. D. Smith, S. H. Payne, E. S. Baker, *Int. J. Mass Spectrom.* **2018**, *427*, 91–99.
- [60] A. A. J. Wei, A. Joshi, Y. Chen, J. S. McIndoe, *Int. J. Mass Spectrom.* **2020**, *450*, 116306.
- [61] E. Janusson, A. V. Hesketh, K. L. Bamford, K. Hatlelid, R. Higgins, J. S. McIndoe, *Int. J. Mass Spectrom.* **2015**, *388*, 1–8.
- [62] S. Nekkanti, N. P. Kumar, P. Sharma, A. Kamal, F. M. Nachtigall, O. Forero-Doria, L. S. Santos, N. Shankaraiah, *RSC Adv.* **2016**, *6*, 2671–2677.
- [63] Q. Michaudel, D. Thevenet, P. S. Baran, *J. Am. Chem. Soc.* **2012**, *134*, 2547–2550.
- [64] S. Sathyamoorthi, Y. H. Lai, R. M. Bain, R. N. Zare, *J. Org. Chem.* **2018**, *83*, 5681–5687.
- [65] C. Vicent, D. G. Gusev, *ACS Catal.* **2016**, *6*, 3301–3309.
- [66] E. Pedrajas, I. Sorribes, K. Junge, M. Beller, R. Llusar, *ChemCatChem* **2015**, *7*, 2675–2681.
- [67] Z. Ahmadi, L. P. E. Yunker, A. G. Oliver, J. S. McIndoe, *Dalton Trans.* **2015**, 44, 20367–20375.
- [68] H. C. Johnson, R. Torry-Harris, L. Ortega, R. Theron, J. S. McIndoe, A. S. Weller, *Catal. Sci. Technol.* **2014**, *4*, 3486–3494.
- [69] Z. Ahmadi, A. G. Oliver, J. S. McIndoe, *ChemPlusChem* **2013**, *78*, 632–635.
- [70] I. Sorribes, G. Wienhöfer, C. Vicent, K. Junge, R. Llusar, M. Beller, *Angew. Chem. Int. Ed.* **2012**, *51*, 7794–7798; *Angew. Chem.* **2012**, *124*, 7914–7918.
- [71] D. H. Ringger, I. J. Kobylanski, D. Serra, P. Chen, *Chem. Eur. J.* **2014**, *20*, 14270–14281.
- [72] J. Luo, A. G. Oliver, J. S. McIndoe, *Dalton Trans.* **2013**, 42, 11312.
- [73] Z. Ahmadi, J. S. McIndoe, *Chem. Commun.* **2013**, 49, 11488.
- [74] J. B. C. Mack, K. L. Walker, S. G. Robinson, R. N. Zare, M. S. Sigman, R. M. Waymouth, J. Du Bois, *J. Am. Chem. Soc.* **2019**, *141*, 972–980.
- [75] L. P. E. Yunker, Z. Ahmadi, J. R. Logan, W. Wu, T. Li, A. Martindale, A. G. Oliver, J. S. McIndoe, *Organometallics* **2018**, *37*, 4297–4308.
- [76] M. A. Henderson, J. Luo, A. Oliver, J. S. McIndoe, *Organometallics* **2011**, *30*, 5471–5479.
- [77] X. Hua, J. Masson-Makdissi, R. J. Sullivan, S. G. Newman, *Org. Lett.* **2016**, *18*, 5312–5315.
- [78] P. S. Fier, J. Luo, J. F. Hartwig, *J. Am. Chem. Soc.* **2013**, *135*, 2552–2559.
- [79] A. J. Ingram, K. L. Walker, R. N. Zare, R. M. Waymouth, *J. Am. Chem. Soc.* **2015**, *137*, 13632–13646.
- [80] M. Kolter, K. Koszinowski, *Chem. Eur. J.* **2019**, *25*, 13376–13384.

- [81] R. G. Belli, Y. Wu, H. Ji, A. Joshi, L. P. E. Yunker, J. S. McIndoe, L. Rosenberg, *Inorg. Chem.* **2019**, *58*, 747–755.
- [82] D. D. Marshall, R. Powers, *Prog. Nucl. Magn. Reson. Spectrosc.* **2017**, *100*, 1.
- [83] R. M. Gathungu, R. Kautz, B. S. Kristal, S. S. Bird, P. Vouros, *Mass Spectrom. Rev.* **2020**, *39*, 35–54.
- [84] D. Yeung, J. Penafiel, H. S. Zijlstra, J. S. McIndoe, *Inorg. Chem.* **2018**, *57*, 457–461.
- [85] A. Joshi, H. S. Zijlstra, S. Collins, J. S. McIndoe, *ACS Catal.* **2020**, *10*, 7195–7206.
- [86] C. Iacobucci, S. Reale, F. De Angelis, *Angew. Chem. Int. Ed.* **2016**, *55*, 2980–2993; *Angew. Chem.* **2016**, *128*, 3032–3045.

---

Manuscript received: July 20, 2021  
Version of record online: December 15, 2021

---